Complex Index of Refraction of Multi-walled Carbon Nanotubes in Strong Terahertz Fields

Oregon State University
Department of Physics

Dalton McCuen

May 26, 2015

Advisor: Dr. Yun-Shik Lee

Abstract

Carbon nanotubes are the subject of intense interest in virtually every field, from medicine to nano-scale electrical components. Multi-walled nanotubes exhibit a strong nonlinear response to high-field strength terahertz radiation. This research uses terahertz pulses with field strength exceeding 1 MV/cm generated by means of optical rectification utilizing a lithium niobate prism to determine the complex refractive index of free standing highly aligned multi-walled carbon nanotubes wound around a polyethylene reel. Computational techniques are used to determine the index of refraction and extinction coefficient simultaneously as a function of frequency.

Contents

1 Introduction

Carbon nanotubes have been subject to widespread scientific study since their invention due to their unique mechanical and electrical properties. Specifically, there has been much interest in the use of carbon nanotubes (CNTs) to create field-effect transistors [5], medical applications [3], and for optical limiting applications [6] among countless other prospective applications. Here we utilize a reliable means of material parameter extraction to determine the complex index of refraction of multi-walled carbon nanotubes (MWCNTs) in the presence of strong terahertz pulses.

1.1 Carbon Nanotubes

CNTs consist of single layers of graphene rolled into a tube shape. They may be single-single walled, consisting of just one rolled sheet, or multi-walled, having multiple tubes nested within one another [4]. One of the more interesting properties of CNTs is their high carrier mobility (on the order of 10 cm^2 V^{-1} s^{-1} or higher)[9]. CNTs exhibit nonlinear behavior when exposed to high field terahertz radiation. The samples analyzed were multi-walled, and were wound repeatedly around a metal reel, the result of which is very precise alignment of the tubes. The reel wound MWCNTs were characterized by finding their complex refractive index over the range from 0.5 to 1.5 terahertz, at a relatively high field strengths, on the order of megavolts per centimeter.

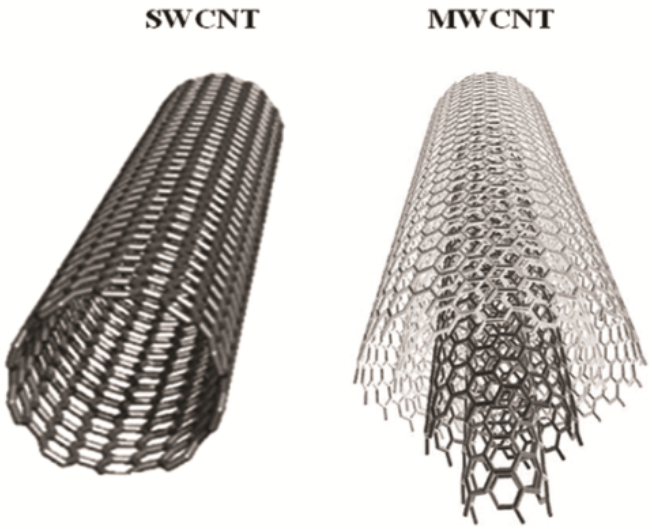

Figure 1: Single- and multi-walled carbon nanotubes. The nanotubes used in this experiment have on average 9 walls per tube.

1.2 Terahertz Radiation

The terahertz portion of the electromagnetic spectrum has been a popular subject of study for several years due to recent advances in the production of pulses at the proper frequencies [7],[2]. The terahertz pulses used in this experiment were created by optical rectification of tilted optical pulse fronts, a common method of generating terahertz pulses [10],[8].

1.3 Complex Index of Refraction

Index of refraction is usually represented by a complex number $\tilde{n}$ whose two components are called the index of refraction and the extinction coefficient. The two components respectively characterize the effective speed of light in the material and rate of absorption of the light by the medium. Both components of the index of refraction are material properties that are frequency dependent, so to fully characterize a material the index must be determined over an entire spectrum. This report focuses on the terahertz portion of the spectrum, using strong terahertz pulses. By measuring transmission of these pulses through the nanotubes sheets the refractive index and absorption coefficient are determined simultaneously, using previously established computational methods [1].

2 Theory

2.1 Index of Refraction

Allowing the index of refraction to be complex ($n \to \tilde{n} = n_R + in_I$), and using the complex number formalism to write an electromagnetic wave as follows

$$\vec{E} = \vec{E}_0 \cos(\omega(t - \frac{\tilde{n}}{c}y))$$
$$\vec{E} = \vec{E}_0 \left[e^{i\omega(t-\frac{\tilde{n}}{c}y)}\right]$$
$$\vec{E} = \vec{E}_0 e^{i\omega(t-\frac{n_R}{c}y)} e^{-\omega\frac{n_I}{c}y}$$

The first exponential is the result obtained if the index of refraction is assumed to be real. The second exponential term indicates that the amplitude falls off exponentially with the depth the wave penetrates into the material. The intensity of a wave is dependent on the square of it is amplitude, so it may be written that

$$I(y) = I_0 e^{-2\omega\frac{n_I}{c}y}$$
$$I(y) = I_0 e^{-\alpha y}$$

where $\alpha = 2\omega\frac{n_I}{c} = 4\pi\frac{n_I}{\lambda_0}$ is the previously mentioned absorption coefficient. It has units of inverse meters, and is an important characteristic of any material. The reciprocal of the attenuation coefficient is called the penetration depth, and it is the depth at which a wave's intensity is $\frac{1}{e}$ times the incident intensity.

2.2 Fabry-Perot Effect

The Fabry-Perot effect (FP) is the result of the multiple reflections between parallel interfaces of different materials. In this experiment, the terahertz pulses pass through two MWCNT sheets, so the FP effect must be accounted for inside both sheets in addition to in the space between them.

Consider a beam of light with electric field strength E_I incident normally on an object with parallel sides sandwitched between two areas having a different index of refraction, as in Figure 2. The field strength of the first transmitted beam (the one which reflects internally zero times) $E_T^{(0)}$ is given by

$$E_T^{(0)} = E_I T e^{i\phi_l}$$

where $T = t_1 t_2$, with $t_1 = \frac{2\tilde{n}_1}{\tilde{n}_2+\tilde{n}_1}$ and $t_2 = \frac{2\tilde{n}_2}{\tilde{n}_2+\tilde{n}_1}$ being the transmission coefficients at the first and second interfaces, and $e^{i\phi_l}$ accounting for the absorption over a distance traversed in the medium l. The second, third, and n^{th} transmitted beams have magnitudes given by

$$\begin{aligned} E_T^{(1)} &= E_I T e^{i\phi_l} R e^{i2\phi_l} \\ E_T^{(2)} &= E_I T e^{i\phi_l} R^2 e^{i4\phi_l} \\ &\vdots \\ E_T^{(n)} &= E_I T e^{i\phi_l} R^{(n)} e^{i2(n)\phi_l} \end{aligned}$$

where $R = r^2$, with $r = \frac{\tilde{n}_2-\tilde{n}_1}{\tilde{n}_2+\tilde{n}_1}$ and $e^{i2m\phi_l}$ accounting for the absorption over a distance traversed in the medium $2ml$. The total transmitted field is equal to the superposition of the transmitted beams that reflected every possible number of times.

$$\begin{aligned} E_T &= \sum_{m=0}^{\infty} E_T^{(m)} \\ E_T &= \sum_{m=0}^{\infty} E_I T e^{i\phi_l} R^{(m)} e^{i2(m)\phi_l} \\ E_T &= E_I T e^{i\phi_l} \sum_{m=0}^{\infty} \left(R e^{i2\phi_l} \right)^{(m)} \end{aligned}$$

Evaluate the sum of the geometric series to write the total transmission as

$$E_T = \frac{E_I T e^{i\phi_l}}{1 - R e^{i2\phi_l}} \tag{1}$$

Applying exactly the same analysis inside each CNT layer as well as in the space between leads to a total transmission function in terms of the index of refraction of the CNT layers.

2.3 Error Functions

To determine simultaneously the index of refraction and the extinction coefficient, consider a theoretical function of the transmission based on the transmission coefficients and the FP effects that is dependent on the index of refraction. By minimizing the difference between the mathematical model and the measured transmission, the values for both the real and imaginary part of the index of refraction can be determined simultaneously. The problem is that the transmission function could be oscillatory with respect to either part of the refractive index. To solve the problem, construct a function that is smooth and monotonous in both n_R and n_I. Both the natural log of the amplitude of the transmission and the argument of the transmission are such functions.

$$\delta\rho = \ln\left(\frac{|T(\omega)|}{|T_{measured}(\omega)|} \right) \tag{2}$$

$$\delta\phi = \arg\left(T(\omega)\right) - \arg\left(T_{measured}(\omega)\right) \tag{3}$$

and the combined function

$$\delta(n_R, n_I) = \delta\rho^2 + \delta\phi^2 \tag{4}$$

where each of the summands are squared so that their relative signs do not lead to false minima of the error function. These functions are referred to as "error functions" from here on, not

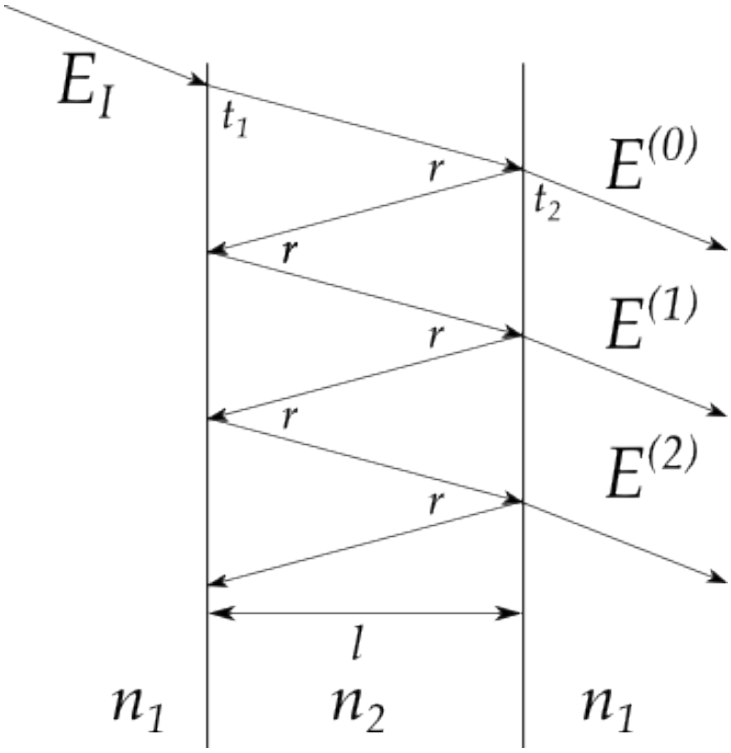

Figure 2: Fabry-Perot Effect. The transmission through each layer of the sample is a superposition of the beams that bounce back and forth inside the medium an arbitrary number of times.

to be confused with the Gaussian error function used in statistics. These functions are so named because they provide a measure of the "error" between the theoretical prediction and the measured transmission. The combined error function (equation 4), an example of which can be seen in figure 3, can then easily be used to find the complex refractive index, as outlined in the methods section below.

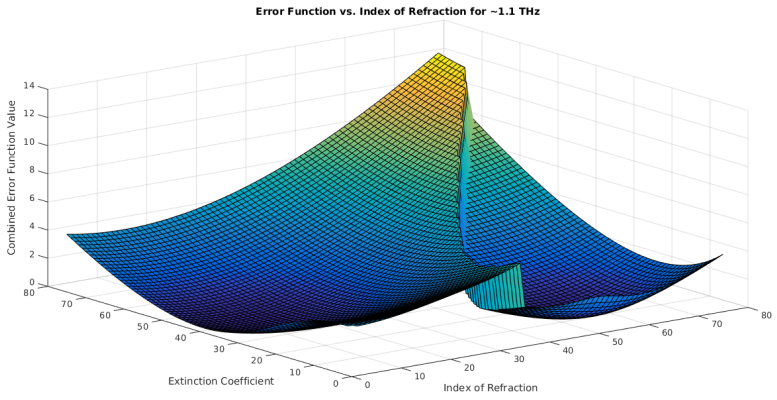

Figure 3: The combined error function at $f = 1.1$ THz. There are two local minima in the combined function when both index components are positive, and six more for negative values. A carefully chosen starting point is used in the algorithm that finds the minimum at each frequency, such that the minimum with physical significance is returned.

3 Methods

3.1 Terahertz Generation and Sample Exposure

The terahertz pulses used in this experiment are generated by optical rectification [10]. A titanium sapphire laser system generates 100 fs pulses centered around 800 nm. These optical pulses are bounced off of an angled diffraction grating, creating a train of angled pulse fronts as shown in figure 4. When these pulse fronts pass through the lithium niobate prism, they emerge as pulses in the terahertz band, with a spectrum centered around 0.8 terahertz. From there the terahertz pulse travels to the MWCNT sample.

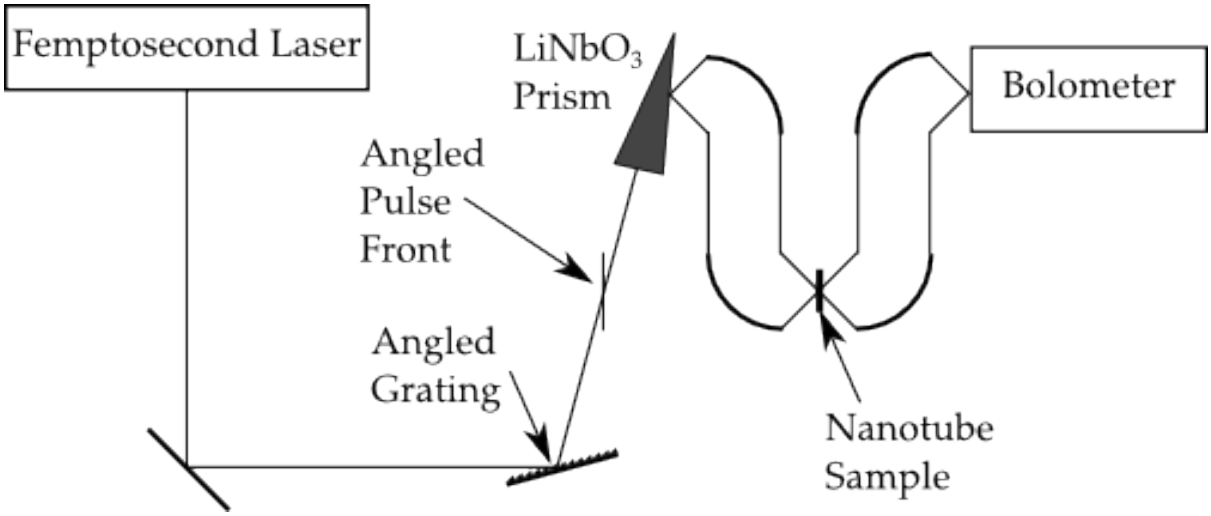

Figure 4: Terahertz pulse generation scheme. 800 nm angled pulse fronts are transformed into terahertz pulses after travelling through a lithium niobate prism. The transmitted electric field is measured by a silicon bolometer.

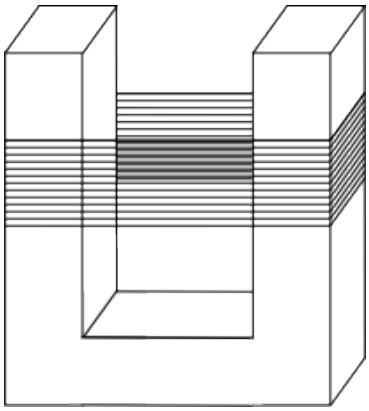

Figure 5: Multi-walled carbon nanotubes wound about a polyethylene reel. This method of fabrication results in a very high degree of alignment of the nanotubes.

The sample consists of CNTs wound repeatedly around a small polyethylene fork, such that subsequent winds are all parallel to one another, as shown in figure 5. This ensures that the terahertz pulse's polarization is wholly parallel to all of the nanotubes. After passing through the sample, the intensity of the beam is measured with a liquid-helium cooled silicon bolometer. The silicon wafer inside the bolometer heats up, causing measurable changes in conductivity

that indicate the strength of the incident radiation.

3.2 Finding the Complex Index of Refraction

With the previously collected time domain spectroscopy (TDS) transmission data, we can proceed to find the index of refraction and extinction coefficients. The computational technique in use has its origins in the method described in [1]. By minimizing equation 4 simultaneously determine the index of refraction and the extinction coefficient for a particular frequency. By iterating this process over all the frequencies present, the index of refraction and extinction coefficient may graphed over the entire spectrum of our terahertz pulse.

The theoretical transmission is constructed by applying 1 for each layer of the sample. The beam passes into a CNT layer from air and back out into air twice, so the factor of T appears twice in equation 5. The exponential in the numerator accounts for the phase shift as the wave propagates through all three regions. The three terms in the denominator account for the Fabry-Perot effect in all three sections, twice in CNT sheets and once in the space between them.

$$E_T = E_I \frac{T^2 e^{i(2\phi_l + \phi_l')}}{\left(1 - Re^{i2\phi_l}\right)^2 \left(1 - Re^{i\phi_l'}\right)} \tag{5}$$

Now that the form of the transmission equation is known, it can be fleshed out with the expressions for T, R, and ϕ_l and ϕ_l'. After substituting and simplifying, we arrive at equation 6.

$$E_T = \frac{E_I 16\tilde{n}^2 e^{i\frac{\omega}{c}(2\tilde{n}l + l')}}{(\tilde{n}+1)^4 \left(1 - \left(\frac{\tilde{n}-1}{\tilde{n}+1}\right)^2 e^{i2\tilde{n}\frac{\omega}{c}l}\right)^2 \left(1 - \left(\frac{\tilde{n}-1}{\tilde{n}+1}\right)^2 e^{i2\frac{\omega}{c}l'}\right)} \tag{6}$$

With the equation in its final form, the modulus and argument may be used as inputs for the error functions derived in the theory section, equations 2, 3. Then Matlab is used to minimize this two dimensional function for each of the discreet frequency components in the spectrum of our terahertz pulse.
The error function depends on both the index of refraction and the extinction coefficient. When graphed, it takes on the form of a paraboloid as in figure 3. The minimum of the paraboloid indicates the values of the index of refraction and extinction coefficient at the frequency used to create the graph.

4 Results and Discussion

The TDS measurements yielded the terahertz pulses shown in figure 6.

This data was then fourier transformed. These transforms are also shown in figure 6. Next the spectral transmission relative to air was computed, this is shown in figure 7.

The results of minimizing equation 4 are displayed in figure 8. There are still some kinks to work out, this graph is not final (the results are unphysical).

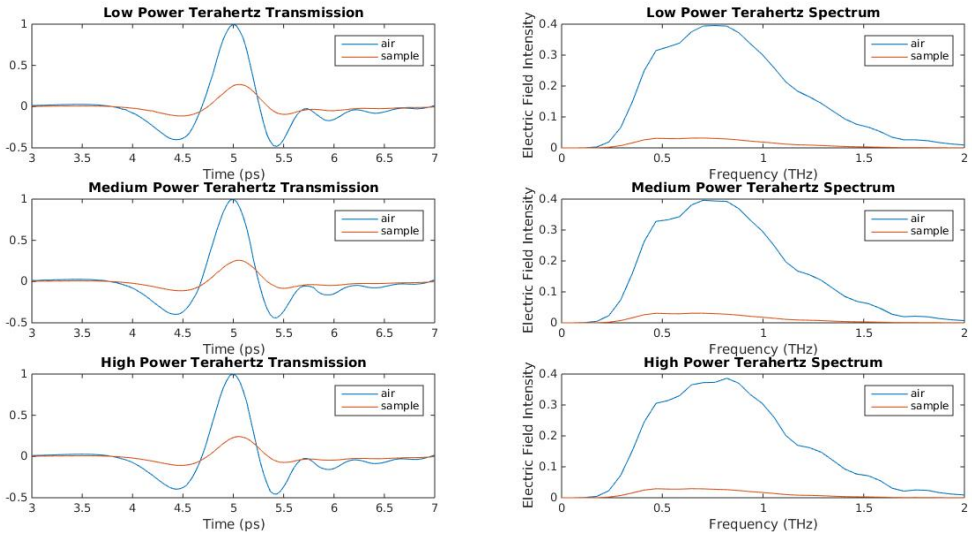

Figure 6: Time and Frequency Domain Data. These graphs indicate that for each power level, the largest spectra transmission occurs between 0.5 and 1.5 terahertz.

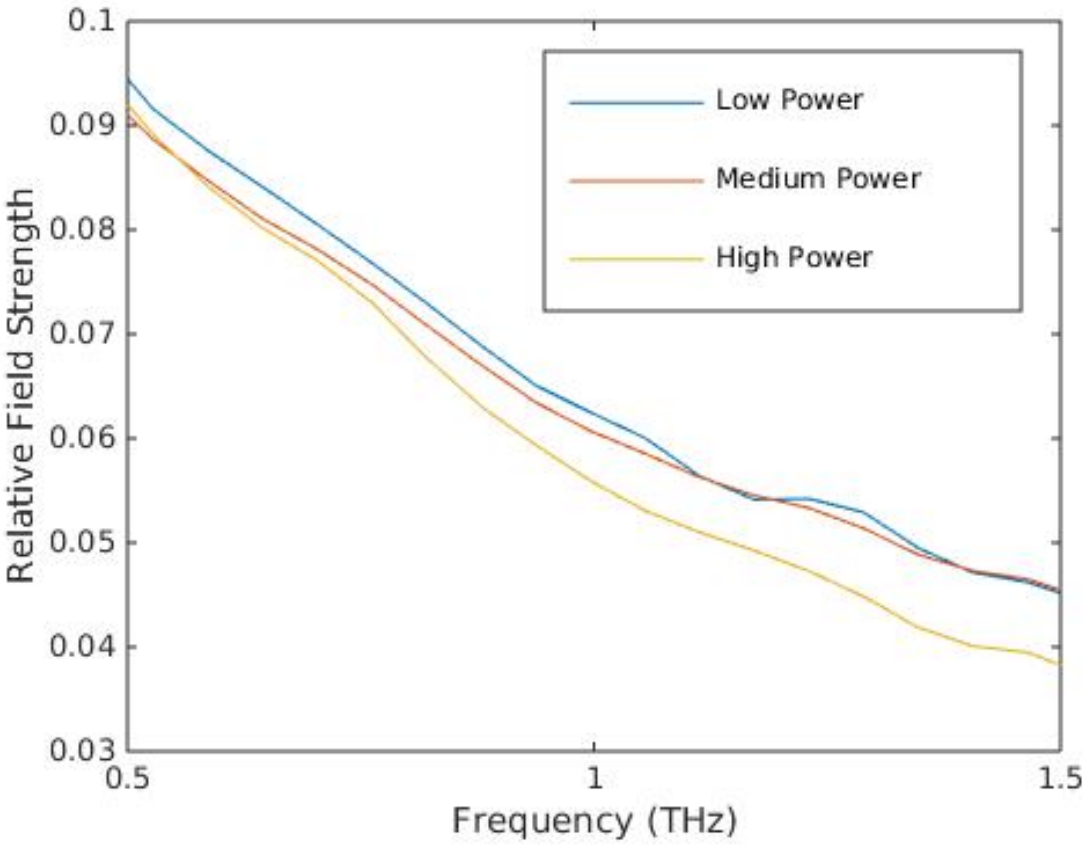

Figure 7: Spectral Transmission Relative to Air. This shows that all three power levels follow the same general general trend, and all are transmitted with nearly the same relative strength. Note that the high power beam is more attenuated than the other two at higher frequencies.

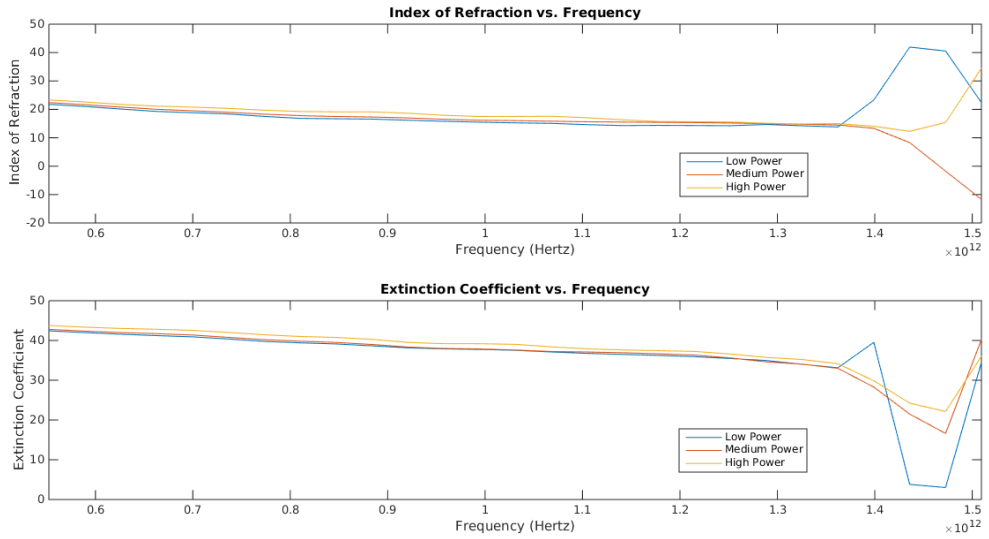

Figure 8: Index of Refraction vs. Frequency. Both graphs follow an obvious downward trend, with the index of refraction and the extinction coefficient decreasing with increasing frequency.

These results resemble those that were expected, but there are some problems. First of all, the values determined are lower than expected, which may suggest that the model used for the transmission through the sample may be flawed or incomplete. Secondly, the data becomes erratic at higher frequencies. This behavior becomes worse at higher and higher frequencies. This is most likely a fault in the minimization method used. It is possible that more advanced techniques would be able to avoid such inconsistent results. However, we can still glean important information from the trends in the data.

5 Conclusion

In this report we were nearly successful in identified the index of refraction and extinction coefficient for parallel multi-walled carbon nanotubes, from 0.5 terahertz up to 1.5 terahertz. The results show that both quantities are dependent upon the amplitude of the applied electric field, demonstrating how the electrical and optical properties of carbon nanotubes may be altered and controlled by application of varying electric field strength. This is a promising result, as it suggests that these applications may soon be realized. They also show that the index of refraction and the extinction coefficient decrease with increasing frequency, a result which agrees with our predictions. The shortcomings of this report indicate that a more sophisticated method of minimizing the error functions is needed, or perhaps that a more detailed model is needed to accurately extract the properties of the multi-walled carbon nanotubes used in this experiment.

6 Bibliography

References

[1] Duvillaret L, Garet F, Coutaz J. A reliable method for extraction of material parameters in terahertz time-domain spectroscopy. Selected Topics in Quantum Electronics Vol. 2, NO 3, September 1996.

[2] Wu Z, Wang L, Peng Y, Young A, Seraphin S, Xin H. Terahertz characterization of multi-walled carbon nanotube films. Journal of Applied Physics 103.

[3] Chakrabarti M, Kiseleva R, Vertegel A, Ray SK. Carbon Nanomaterials for Drug Delivery and Cancer Therapy. Journal of Nanoscience and Nanotechnology Vol. 15, Issue 8, August 2015.

[4] Endo M, Kim YA, Muramatsu H, Yanagisawa T, Hayashi T, Dresselhaus MS. The Large-scale Production of Fibrous Carbons and their Applications. New Diamond and Frontier Carbon Technology Vol. 14, Issue 1, 2004

[5] Martel R, Schmidt T, Shea H R, Hertel T, Avouris Ph. Single- and multi-walled carbon nanotube field-effect transistors. Applied Physics Letters Vol 73, Number 17, 26 October 1998

[6] Chen Y, Lin Y, Liu Y, Doyle J, He N, Zhuang X, Bai J, Blau W. Carbon nanotube-based functional materials for optical limiting. Joural of nanoscience and nanotechnology, Vol 7, numbers 4-5, April/May 2007

[7] Bodrov S, Ilyakov I, Shishkin B, Stepanoc A. Efficient terahertz generation by optical rectification in Si-LiNbO3-air-metal sandwich structure with variable air gap. Applied Physics Letters, Vol. 100, Issue 20, May 2012.

[8] Dietze D, Unterrainer K, Darmo J. Dynamically phase-matched terahertz generation. Optics Letters, Vol. 37, Issue 6, 2012.

[9] Wang G, Huang Y. Theoretical study on the combined systems of peanut-shaped carbon nanotubes encapsulated in single-walled carbon nanotubes. Chemical Physics, Vol. 406, 8 October 2012.

[10] Jeong Y-G, Paul M, Kim S-H, Yee K-J, Kim D-S, Lee Y-S. Large enhancement of nonlinear terahertz absorption in intrinsic GaAs by plasmonic nano antennas. Applied Physics Letters, Vol. 103, 2013.